
This manuscript is a preprint and has been submitted for publication. Subsequent versions may have slightly different content. The DOI of the peer reviewed publication will be provided if accepted. Please contact the authors if you have any questions or comments on this manuscript.

1 Plastic plants: Water hyacinths as driver of plastic transport in 2 tropical rivers

3 Authors

4 Louise Schreyers^{1*}, Tim van Emmerik¹, Thanh Luan Nguyen², Evelien Castrop¹, Ngoc-Anh Phung³,
5 Thuy-Chung Kieu-Le^{3,4}, Emilie Strady⁵, Lauren Biermann⁶, Martine van der Ploeg¹

6 ¹Hydrology and Quantitative Water Management Group, Wageningen University, Wageningen, The
7 Netherlands

8 ²École Polytechnique de Montréal, Montréal, Canada

9 ³Ho Chi Minh City University of Technology (HCMUT), Ho Chi Minh City, Vietnam

10 ⁴Vietnam National University Ho Chi Minh City, Ho Chi Minh City, Vietnam

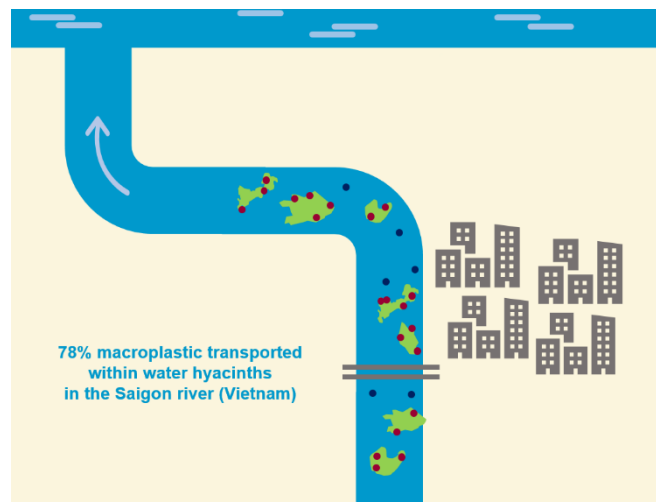
11 ⁵Aix-Marseille University, Mediterranean Institute of Oceanography (MIO), Marseille, Université de
12 Toulon, CNRS/IRD, France

13 ⁶Plymouth Marine Laboratory, Prospect Place, Plymouth, UK

14 *Corresponding author. E-mail: louise.schreyers@wur.nl

16 Abstract

17 Recent studies suggest that water hyacinths
18 play an important role in the transport of
19 macroplastics in freshwater ecosystems.
20 Forming large patches of several meters at
21 the water surface, water hyacinths tend to
22 entrain and aggregate large amounts of
23 floating debris, including plastic items.
24 Research on this topic is still novel and few
25 studies have quantified the role of the water
26 hyacinths in plastic transport. In this study, we
27 present the findings of a six-week monitoring



28 campaign, combining the use of visual observations and aerial surveys in the Saigon river, Vietnam. For
29 the first time, we provide observational evidence that the majority of plastic is transported downstream
30 by water hyacinths. Over the study period, these fast-growing and free-floating water plants transported
31 78% of the macroplastics observed. Additionally, we present insights on the spatial distribution of plastic
32 and hyacinths across the river width, and the different characteristics of entrapped items compared with
33 free-floating ones. With this study, we demonstrate the role of water hyacinths as a river plastic
34 aggregator, which is crucial for improving the understanding of plastic transport, and optimizing future
35 monitoring and collection strategies.

36 **Keywords:** macroplastic; microplastic; riverine pollution; aquatic vegetation; observations; field data

39 Introduction

40 Rapid growth in plastic production and consumption has made plastic pollution an ubiquitous issue
41 across the globe. Plastics can directly harm aquatic and terrestrial species, and cause serious economic
42 damage¹. Alarming, studies predict major increases in plastic emissions due to low recycling rates,
43 global increases in plastic consumption, and difficulties in large scale plastic reduction efforts^{2,3}. Plastic
44 pollution monitoring efforts are being conducted at various scales, but these initiatives focus mostly on
45 marine and coastal areas, rather than riverine ecosystems⁴. Despite rivers assumed to account for the
46 majority of the plastic emitted into oceans⁵, many aspects on plastic transport and fates in river systems
47 remain unknown. Yet, quantifying riverine plastic loads is essential for assessing the efficiency of plastic
48 reduction measures such as reduction of plastic consumption and improving of waste disposal.

49 Understanding of the role of various factors in plastic transport variability in rivers is expanding, and
50 studies are exploring different drivers for different sizes of plastic debris. It is often assumed that
51 hydrometeorological variables are important drivers of plastic flux¹. River discharge was related plastic
52 transport in the Seine, France⁶ and changes in dry/wet seasons correspond to significant plastic debris
53 fluctuations in the Wonorejo river, Indonesia⁷. In the UK, flood events were found to be responsible for
54 microplastic export⁸. Other drivers, such as sediment loads have also been recently examined in
55 Australia⁹, China¹⁰ and Amazonian rivers¹¹ in relation to microplastic transport. Mangrove forests and
56 coastal vegetation habitats can also be an important sink of plastic debris¹²⁻¹⁴. In the Saigon river,
57 Vietnam, macroplastic transport was correlated to the abundance of organic debris (mainly floating water
58 hyacinths), rather than hydrological variables¹⁵. Both the abundance of plastic and water hyacinths were
59 found to vary with an order of magnitude, suggesting hyacinths have a substantial influence on plastic
60 transport. For better understanding of plastic transport dynamics in the (sub)tropics, exploring the role
61 of water hyacinths is thus crucial.

62 Water hyacinth (*Eichhornia crassipes*) is a macrophyte species native from the Amazon, which has
63 spread to most freshwater ecosystems in the tropics and subtropics¹⁶. Water hyacinths are aquatic
64 weeds that tend to aggregate and form large patches floating at the water surface. They are considered
65 one of the most invasive vegetation species in the world, and have already spread to 15 Asian and 36
66 African countries^{17,18}. More recently, these floating water plants have been observed in North America
67 and Southern Europe^{17,19}. Despite water hyacinths being considered a nuisance, their absorbent
68 capacities offer an opportunity to use them as ecological indicators, and their role in the absorption of
69 pollutants such as heavy metals has been well ascertained²⁰. Our interest in hyacinths in relation to
70 plastic pollution is three-fold. Firstly, we hypothesize that hyacinths substantially influence spatio-
71 temporal variation in riverine plastic transport. Understanding this relationship is key for improved plastic
72 transport quantification. Secondly, the detectability of large floating vegetation aggregations from
73 satellite^{16,21,22} is an opportunity to use hyacinth patches as a proxy for plastic pollution. This could be an
74 important step in scaling-up plastic monitoring efforts. Lastly, if the role of hyacinths in aggregating
75 plastic is ascertained, clean-up efforts could utilize the plant as a means for efficient plastic co-removal
76 in inland waters. In this paper, we provide a first assessment of the role of water hyacinths in riverine
77 macroplastic transport. We present findings of a six-week measurement campaign that combined visual

78 observations and aerial surveys. We monitored the contribution of plastic entangled in hyacinths relative
 79 to the total plastic transport, the accumulation of plastics in hyacinths, and composition of plastics within
 80 and outside hyacinths. With this paper we aim to: (1) demonstrate the substantial role of water hyacinths
 81 in plastic transport, and (2) provide insights on the characteristics (polymer composition and size
 82 distribution) of plastics that are transported by hyacinths.

83 **Materials and methods**

84 We focused on the Saigon river, considered the 5th most plastic polluted watershed in Vietnam²³. The
 85 Saigon river is part of the Saigon–Dong Nai river system that traverses Ho Chi Minh City (HCMC). The
 86 Saigon river is controlled upstream by a reservoir and is subjected to diurnal asymmetric tides. Its net
 87 annual water discharge was estimated of 50 m³ s⁻¹, fluctuated monthly from 4 to 222 m³ s⁻¹²⁴. Plastic
 88 pollution in the Saigon river has already been monitored by several studies, thus enabling investigation
 89 of transport dynamics^{15,25}.

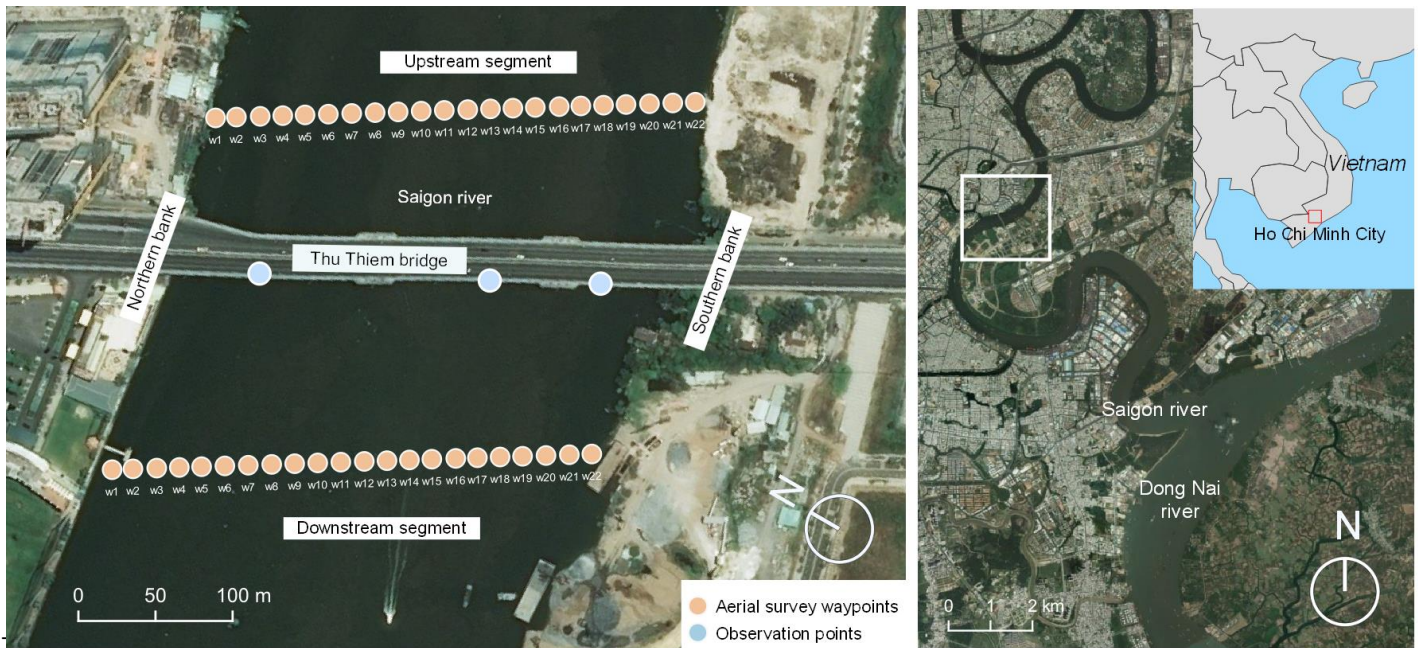
90 We used two complementary measurement methods to quantify both the role of water hyacinths in
 91 plastic accumulation and in transport (table 1). Visual observations enabled to estimate macroplastic
 92 transport flux at the water surface for 15 days. Aerial surveys, on the other hand, allowed finer
 93 characterization on the plastic entangled in water hyacinths, such as spatial distribution along the river
 94 width, polymer composition, item size and plastic density within vegetation patches. Visual counting
 95 could be used for item polymer categorization, but becomes challenging in a context of high plastic
 96 flux²⁵. The aerial survey uses photos and does not allow to calculate flux²⁶.

97 The visual measurement campaign took place between the 27 April to the 8 June 2020. The plastic
 98 items counting protocol was adapted from the methodology developed by van Emmerik et al.²⁵. The
 99 counting was done from the Thu Thiem bridge in HCMC (10°47'08.3"N, 106°43'06.2"E), see fig. 1. The
 100 aerial measurements were taken on the 23 May 2020 only. A total of ten UAV flights were conducted
 101 on that day, with the four initial flights 100 m downstream the bridge, and the six subsequent surveys
 102 80 m upstream. The aerial survey method that we present is similar to the method tested by Geraeds et
 103 al.²⁷, with the alteration of splitting the cross-sectional flights to two locations, due to tidal influences.

104 **Table 1.** Overview of methods used to characterize macroplastic transport and storage in water
 105 hyacinths for the Saigon river

Method	Temporal coverage	Spatial extent per survey	Processing / data analysis	Derived metrics
Visual observation	15 observations of 1 day over a 6-week period	45 m among 340 m of river width	Extrapolation of values for whole river width	# items / min (entangled and free-floating)
Aerial survey	1 day – 23 May	335 m at two nearby river segments (out of 340 m of river width)	Manual labelling and color filtering	# items in and out water hyacinths, items size, polymer composition, distribution along river width, vegetation area, # items /m ²

106



107
 108 **Figure 1.** Localization of visual observation points and 22 aerial survey waypoints. Source: Bing
 109 imagery.

110 **Visual counting for Temporal Plastic Flux**

111 The visual counting method was adapted from van Emmerik et al.^{25,28}. It is a well-established and simple
 112 observation procedure, easily replicable at various locations.

113 The visual observations were conducted from three different locations along the Thu Thiem bridge over
 114 a period of 6 weeks. It is estimated that at each location, the surveyor was able to detect all floating
 115 plastic items along a 15 m width section. Overall, 13% (45 m out of 340 m) of the river cross-section
 116 was covered by the visual counting. The bridge is approximately 14 m above the water level and the
 117 counting was done facing downstream. During a time frame of two minutes and at one bridge location,
 118 the surveyor counted all plastic items within vegetation patches (entangled). This observation sequence
 119 was followed by another 2-minute time frame to count plastic debris located outside (free-floating) of
 120 water hyacinths. If the nature of the debris was uncertain, it was not counted as a plastic item. After the
 121 visual counting at one observation point, the surveyor proceeded to the next one. For each
 122 measurement day, several profile of the bridge were done. Subsequent data analysis included
 123 extrapolation of plastic flux for the whole river width and scaling to obtain hourly values (text S1).

124 **UAV survey**

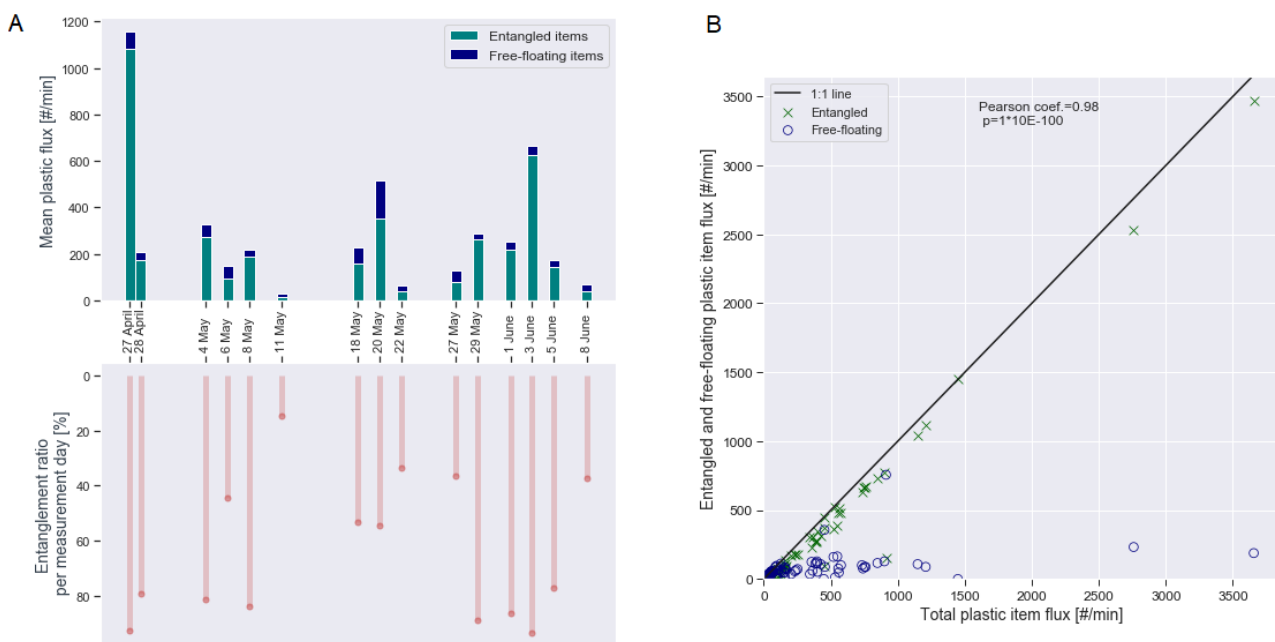
125 A DJI Phantom 4 Pro UAV (DJI, Shenzhen, China; <http://www.dji.com>) was used to acquire aerial
 126 imagery upstream and downstream of the Thu Thiem bridge on 23 May 2020. A total of 3,936 images
 127 were taken at 22 waypoints across the river width. Blurry images were discarded ($n = 261$) and
 128 ultimately, only images with visible plastic items were retained for analysis ($n = 128$). The low number
 129 of images analyzed is due to the removal of overlapping images at the same waypoint. When images
 130 taken at a waypoint showed differences in the number of plastic items, they were both analyzed, making
 131 sure that items present on both images were not counted double.

132 The selected images were manually labelled with the open source Visual Geometry Group Image
 133 Annotator (VIA) tool²⁹. Two categories of plastic were distinguished: “free-floating” items – plastic debris
 134 flowing freely at the river surface – and “entangled” items – plastic waste trapped within hyacinth.
 135 Rectangular polygons were drawn around each identified plastic item for size and area estimates (fig.
 136 S1). Information on the polymer composition was also filled in during the manual labelling. Seven
 137 polymer types were distinguished, following the categorization used in van Emmerik, Strady, et al.¹⁵: (1)
 138 E-PS (expanded polystyrene), (2) PO hard (hard polyolefins), (3) PO soft (soft polyolefins), (4) PS
 139 (polystyrene), (5) PET (polyethylene terephthalate), (6) Multilayer plastics, and (7) Rest plastics. The
 140 items were categorized based on color, shape and other visual properties such as transparency. When
 141 the polymer composition of the item was uncertain, it was categorized as part of the category ‘Rest’.

142 To estimate the aquatic vegetation coverage area, color filtering was performed using the Open CV
 143 library in Python over a selection of images (n = 75) (text S3, fig. S2). Ultimately, the ground sampling
 144 distance was determined, based on the flying elevation, the image width in pixels, sensor width and
 145 focal length of the camera (text S3). This allowed us to estimate both vegetation and plastic item areas.

146 **Results and discussion**

147 **Temporal variability in plastic items transport**



148
 149 **Figure 2.** A. Mean plastic flux and entanglement ratios per measurement day as measured from visual
 150 observations. B. Entangled and free-floating plastic flux in relation to total plastic flux. Each data point
 151 represents one visual counting observation.

152 Estimated mean plastic flows show large temporal variability during the visual counting period. Mean
 153 daily plastic flux calculated from visual observations varied between 15 to 1,080 items/minute (fig.2A),
 154 with the lowest mean plastic flux on 11 May and peak mean plastic flux on 27 April. No steady and

155 consistent temporal trend is noticeable over the 6-week period: days with low plastic flux can be followed
156 by increases in plastic flux and then register a significant drop at the next measurement day.

157 The entrapped fraction of transported macroplastic varies greatly, from 15% to 93% depending on the
158 measurement day (fig.2A), with days registering low ratios broadly corresponding to low plastic daily
159 flux (6 May, 11 May, 22 May, 27 May, 8 June). In addition, we found that plastic transported by hyacinths
160 shows a variability in mean flux of three orders of magnitude (2-1,002 items/min). This is considerably
161 higher than the variability in free-floating flux, of one order of magnitude (12-160 items/min). These
162 results suggest that the transport of plastic entrapped in hyacinths has a major influence on the total
163 plastic transported along the river.

164 During the 6-week period of visual counting, water hyacinths transported an average of 78% of the
165 observed plastic items. The mean plastic flux over the study period was estimated at 170 items/min for
166 entangled items and 48 items/min for free-floating debris. Total mean plastic flux was thus approximately
167 of 218 items/min.

168 We found a highly positive correlation between entangled plastics and total plastic items (fig. 2B), the
169 latter being likely mainly driven by the amount of hyacinths flowing. Data on the transport of free-floating
170 items, on the other hand, show a lower positive correlation ($r = 0.48$, $p < 0.01$) with total plastic flux.
171 These results suggest that total plastic transport in the Saigon River flanking Ho Chi Minh City is mainly
172 driven by plastics accumulated in hyacinths.

173 For the month of May specifically, we estimate a total plastic flux of 162 items/min. Interestingly, this
174 estimation is close to the mean flux values (117-133 items/min) found by van Emmerik, Strady, et al.¹⁵
175 for May 2018 at the same location. The slightly higher flux that we measured in 2020 might be
176 attributable to variability in environmental drivers (for example, rainfall for water flow, temperature for
177 hyacinth growth), increases in plastic consumption, mismanagement and leakage between observed
178 years, and to the lower number of observation points along the bridge for the visual counting in 2020.
179 Higher transport flux at the location of the observation points compared to the rest of the river might
180 have induced an overestimation of plastic flux along the river width. We recommend to proceed to visual
181 counting at more locations in the future, for improved accuracy in the plastic transport estimates.

182 **Spatial distribution of plastic debris and water hyacinths**

183 The spatial distribution of plastic debris and vegetation captured by the UAV survey on 23 May shows
184 large heterogeneity in hyacinth and plastic concentrations along the river width, with clear accumulation
185 zones. For aerial surveys done downstream of the bridge, debris and vegetation patches accumulated
186 in largest amounts close to the northern river bank at waypoint 1. Approximately 57% of detected
187 hyacinth patches, 40% of plastic items entangled in hyacinth, and 33% free-floating items were observed
188 along the first 35 m from the northern river bank (fig.3A). Vegetation and plastic concentration zones
189 were also observable at 80 m (waypoint 6) from the north river bank, and waypoint 16 at 230 m (closer
190 to the southern river bank). For the section upstream of the bridge, concentration near the northern river
191 bank is even higher (fig.3A). Most plastic items accumulated in the first 35 m from the north river bank
192 (87% for entangled items and 74% for free-floating ones), with just a few items counted at waypoint 16

193 covering 230-275 m. The hyacinths were all concentrated at the northern bank for the upstream surveys.
194 This can be explained by the higher number of plastic items detected over the 7th flight (n = 193)
195 compared to the average number of detected items for all other flights (n = 40).

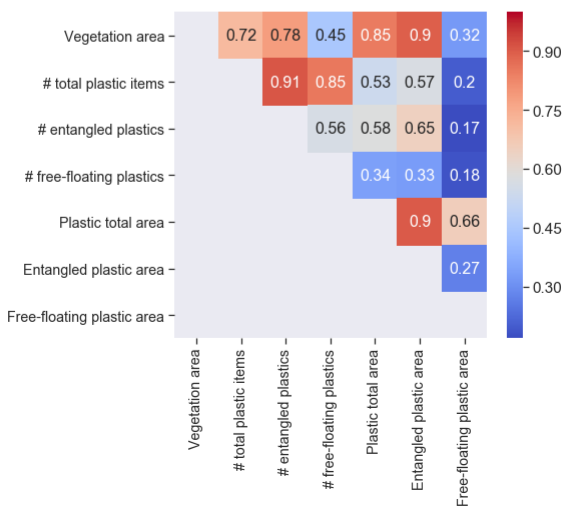
196 Overall, it remains unclear if the observed distribution pattern is the result of the absence of hyacinths
197 in the mid-channel sections (given that this section of the river is heavily navigated) or if northern
198 sections are natural accumulation zones due to the combined influence of flow velocity, wind speed,
199 river shape and the presence of hyacinths. Understanding what determines the spatial distribution of
200 the water hyacinths could provide new insights on macroplastic accumulation zones and thus inform
201 plastic removal measures.

202

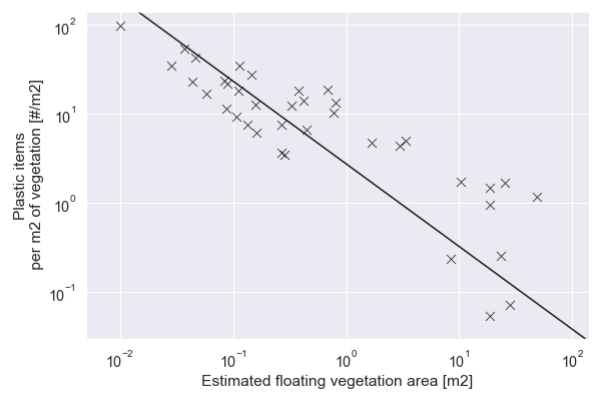
A



B



C



203

204

205

206

207

208

209

210

211

Figure 3. (A) Distribution of vegetation and macroplastics along the river width [%] upstream and downstream the bridge. (B) Correlation matrix of measured metrics. Red shows highest correlation scores between variables, while blue shows lower scores. All p-values are < 0.01 so all correlation scores show significant relationships between variables. (C) Plastic accumulation within hyacinth patches: number of plastic items per m² of vegetation in relation to the estimated vegetation area in m².

For the entire river width, the aerial survey found that 39% (n = 313) of plastic were accumulated in hyacinth on the 23rd of May. Considering only items of a size > 2.5 cm, the entrapment rate rose to 44%.

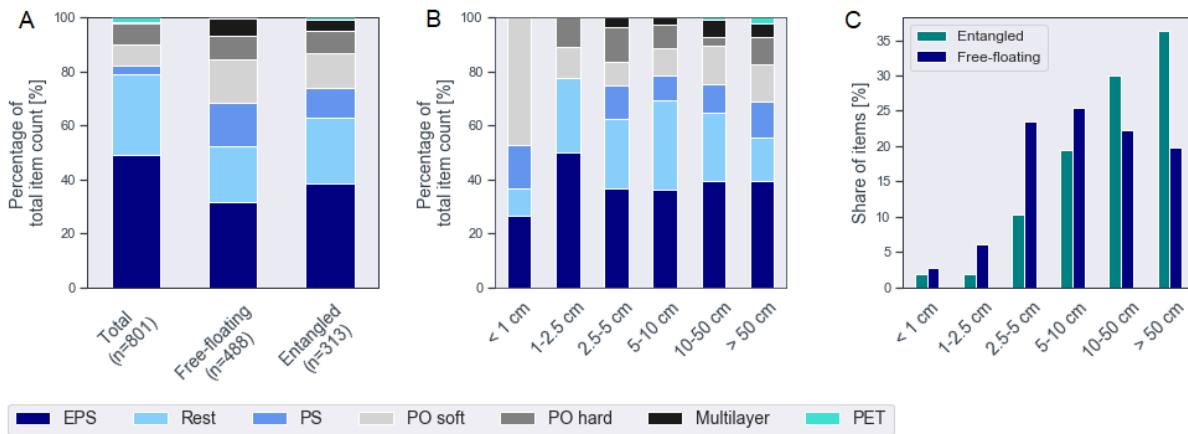
212 Note that this 'snapshot' entanglement ratio cannot be compared directly with the ratio of entangled
213 plastic flux measured over 6 weeks. Nonetheless, the UAV results on spatial distribution are consistent
214 with the visual counting results on transport temporal variability: lower total transport flux on 22 and 27
215 May plus higher free-floating plastic transport compared with hyacinth-entangled flux.

216 Overall, the data (fig.3B) show that the spatial macroplastic distribution is strongly correlated with the
217 hyacinth presence ($r = 0.72$ for the total plastic count and $r = 0.85$ for plastic area) as well as with
218 entrapped plastics ($r = 0.78$ for items count and $r = 0.9$ for area). Furthermore, the area of entangled
219 items is correlated to the size of the hyacinth patch ($r = 0.90$).

220 The accumulation of plastic in vegetation patches varies considerably, from 0 to 98 items per m^2 (fig.
221 3C). On average, the accumulation density is 7 items per m^2 of vegetation. Interestingly, the data show
222 that largest vegetation patches have lowest plastic accumulation densities. Visual examination of the
223 aerial imagery showed that plastic litter is mostly entrapped at the edges of the patches, with a sparser
224 presence of items in the central area. This could indicate that free-floating items interact with the edges
225 of the vegetation patches during their transport.

226 **Polymer composition and size distribution**

227 The plastic debris we detected in UAV imagery consisted mainly of E-PS (38%), in similar proportions
228 compared to previous studies conducted in the Saigon river¹⁵. The predominance of E-PS is the result
229 of both the extensive use of single-use food containers in Vietnam³⁰ as well as the high buoyancy and
230 floatability of this low-density polymer type. E-PS made up for 32% of free-floating items and almost
231 49% of entangled items (fig.4A). Its low density might explain how and why it becomes entrained in
232 hyacinth patches. Hyacinth appears to entangle PET items at higher rates compared with the proportion
233 observed in open water, possibly because the items we observed in the UAV imagery were of a larger
234 size (> 10 cm). Overall, PET were the least abundant (2%) polymer category, a likely effect of re-use or
235 recycling mechanisms targeting this category of plastic debris. The share of items classified as 'Rest' is
236 higher (30%) within the hyacinth patches than outside (21%). Poor identification of entangled plastic
237 materials were likely caused by the partial coverage of plastic debris by leaves and roots. PS, PO soft
238 and Multilayer items were more frequently observed as free-floating debris (respectively, 16, 16 and 6%)
239 than entangled (3, 8 and 1%), indicating that bags and foil items are not easily entrained/ entangled.
240 This may be due to the fact that PO soft items were predominantly below 1 cm in size, suggesting a
241 higher level of fragmentation (fig 4B). Only PO hard particles were found in similar proportions in both
242 entangled and free-floating items (respectively 8 and 9%). This is a considerably lower estimate than
243 found in previous studies, where PO hard accounted for approximately 20% of detected items¹⁵.
244 Possible explanations for this could be observer bias from the manual labelling, or a relative scarcity of
245 PO hard items during the measurement day (23 May). Given that plastic composition is subject to
246 temporal variability¹⁵, higher temporal coverage and frequency on the polymer composition of entangled
247 plastic items is needed to inform plastic reduction strategies.



248

249 **Figure 4.** Polymer composition of plastic items (A), in relation to size categories (B) and overall size
 250 distribution (C).

251 Overall, the hyacinths entrapped larger particles than otherwise observed in open-water (fig.4C). Around
 252 two-third of plastic debris within vegetation patches exceeded 10 cm in size, whereas two-third of free-
 253 floating debris were smaller than 10 cm. There are two possible explanations for this. The first assumes
 254 that the plastic items have been flowing freely for some distance. During their transportation, the large
 255 items get trapped in the vegetation patches, due to contact and interference. On the contrary, the small
 256 debris items appear to be more mobile on the water surface, and perhaps more influenced by flow. The
 257 second explanation considers that most of the plastic litter is leaked into the river system via the
 258 vegetation patches. Indeed, hyacinth are often located close to the riverbanks, where waste may be
 259 more conveniently dumped. Some items then fragment into smaller particles, disentangle from the
 260 hyacinths, and enter the open water. A coupling of these accumulation-transport patterns is not to be
 261 excluded.

262 **Synthesis**

263 This study provides the first observational evidence that water hyacinths have a considerable impact on
 264 riverine plastic transport. Important temporal variations in plastic fluxes of several orders of magnitude
 265 were observed, highlighting the need for long-term continuous plastic monitoring. The importance of
 266 seasonal variability in macroplastic transport in the Saigon river, as already highlighted by van Emmerik,
 267 Strady, et al.¹⁵, prompts for investigations into the seasonality of water hyacinths and its role in plastic
 268 flux variability. We recommend that further research efforts focus on large-scale detection of floating
 269 vegetation, using Earth Observation (EO) satellites. Research shows that floating patches of hyacinth
 270 as well as plastics are detectable from space^{22,31}. The disintegration and growth cycles of hyacinths
 271 could also explain sudden peaks in plastic emitted into the oceans, but have yet to be studied.

272 Further quantification of the macroplastic flux transported in water hyacinths at different seasons is
 273 needed. We found large temporal variations in the ratio of entangled macroplastic (from 15 to 93%),
 274 with high ratios correlating with peaks in plastic transport. Our measurement campaign lasted six weeks
 275 and took place between the end of April and the beginning of June, a season which marks the transition
 276 from the high plastic loads of the dry season to the relatively low plastic flux characteristics of the wet

277 months¹⁵. Longer field measurement campaigns could provide more accurate estimates of the average
278 flux transported by hyacinth, which could then be used as a proxy indicator for estimating plastic
279 transport and emissions.

280 Monitoring efforts may also be expanded to other locations along the Saigon river to better understand
281 plastic transport-sink patterns. Our study focused on one location, but the role of hyacinth may differ in
282 upstream and downstream river segments. Furthermore, it is unclear if the plastic debris is introduced
283 at HCMC or further upstream. Better understanding of the plastic input sources is required for a
284 comprehensive monitoring scheme. Investigating other river systems is also crucial to ascertain whether
285 the dominant role of floating vegetation in plastic transport is specific to the Saigon river or not. Given
286 the high overlap between rivers that have been invaded by hyacinth and rivers that are polluted by
287 plastics, we hypothesize that hyacinth may be a driving force of plastic emission into the ocean in many
288 other watersheds.

289 In our study, we showed that plastic transport is mainly driven by the presence of hyacinths. However,
290 it is possible that in certain configurations – for instance large floating patches on the riverbanks - the
291 hyacinths act more as a barrier for dispersion than a means of transport. Recent studies prove the role
292 of mangrove forests in trapping anthropogenic litter in estuarine¹² and coastal environments^{13,32}. Focus
293 on the residence time, and spatial interactions between hyacinths and plastic and degradation rates
294 could be beneficial in that sense. The routes of macroplastic and transport-storage-remobilization
295 patterns related to hyacinth dynamics should certainly be investigated at different scales³³. Again, EO
296 may prove to be a crucial complementary approach for understanding the river system at synoptics
297 scales. Additional field measurements, such as physical sampling, on the other hand, would be
298 necessary for finer characterization of the fate of plastics once entangled in hyacinths.

299 We conclude that water hyacinths play a substantial role in macroplastic transport in the Saigon river,
300 as 78% of the total plastics were found to be transported by hyacinth patches. In addition, the high
301 positive correlation ($r = 0.98$) between entangled plastic and total plastic flux suggests that hyacinths
302 are a substantial driver in spatiotemporal variation of plastic transport. The item composition differs, with
303 larger items and mainly E-PS plastics predominantly associated with hyacinth, and foils and soft bags
304 more likely to be observed as free-floating items. Additional research is required on the scalability and
305 transferability of our findings to other locations along the Saigon, and other river systems worldwide.

306 **Data availability**

307 All data used for this work are uploaded on the 4TU repository. A DOI will be provided upon publication
308 of the final manuscript.

309 **Authors' information**

310 **Corresponding author**

311 *E-mail: louise.schreyers@wur.nl

312 **Note**

313 The authors declare no competing financial interest.

314 **Acknowledgments**

315 The work of LS was supported by NWO Open Mind grant 18127. The work of TvE was supported by
316 the 4TU.Federation Plantenna project. This study is part of the Plastic Plants project, supported by the
317 ESA OSIP program.

318 **References**

- 319 1. Emmerik van, T. & Schwarz, A. Plastic debris in rivers. *WIREs Water* **7**, (2020).
- 320 2. Borrelle, S. B. *et al.* Predicted growth in plastic waste exceeds efforts to mitigate plastic
321 pollution. *Science* **369**, 1515–1518 (2020).
- 322 3. Lau, W. W. Y. *et al.* Evaluating scenarios toward zero plastic pollution. *Science* **369**, 1455–
323 1461 (2020).
- 324 4. Blettler, M. C. M., Abrial, E., Khan, F. R., Sivri, N. & Espinola, L. A. Freshwater plastic pollution:
325 Recognizing research biases and identifying knowledge gaps. *Water Research* vol. 143 416–
326 424 (2018).
- 327 5. Lebreton, L. & Andrady, A. Future scenarios of global plastic waste generation and disposal.
328 *Palgrave Commun.* **5**, 1–11 (2019).
- 329 6. van Emmerik, T. *et al.* Seine Plastic Debris Transport Tenfolded During Increased River
330 Discharge. *Front. Mar. Sci.* **6**, 1–7 (2019).
- 331 7. Kurniawan, S. B. & Imron, M. F. Seasonal variation of plastic debris accumulation in the
332 estuary of Wonorejo River, Surabaya, Indonesia. *Environ. Technol. Innov.* **16**, 100490 (2019).
- 333 8. Hurley, R., Woodward, J. & Rothwell, J. J. Microplastic contamination of river beds significantly
334 reduced by catchment-wide flooding. *Nat. Geosci.* **11**, 251–257 (2018).
- 335 9. He, B. *et al.* Influential factors on microplastics occurrence in river sediments. *Sci. Total*
336 *Environ.* **738**, 139901 (2020).
- 337 10. Liu, Y. *et al.* Effects of anthropogenic discharge and hydraulic deposition on the distribution and
338 accumulation of microplastics in surface sediments of a typical seagoing river: The Haihe
339 River. *J. Hazard. Mater.* **404**, 124180 (2021).
- 340 11. Gerolin, C. R. *et al.* Microplastics in sediments from Amazon rivers, Brazil. *Sci. Total Environ.*
341 **749**, 141604 (2020).
- 342 12. Ivar do Sul, J. A., Costa, M. F., Silva-Cavalcanti, J. S. & Araújo, M. C. B. Plastic debris
343 retention and exportation by a mangrove forest patch. *Mar. Pollut. Bull.* **78**, 252–257 (2014).
- 344 13. Martin, C. *et al.* Exponential increase of plastic burial in mangrove sediments as a major plastic
345 sink. *Sci. Adv.* **6**, eaaz5593 (2020).

- 346 14. Cozzolino, L., Nicastro, K. R., Zardi, G. I. & de los Santos, C. B. Species-specific plastic
347 accumulation in the sediment and canopy of coastal vegetated habitats. *Sci. Total Environ.*
348 **723**, 138018 (2020).
- 349 15. van Emmerik, T., Strady, E., Kieu-Le, T. C., Nguyen, L. & Gratiot, N. Seasonality of riverine
350 macroplastic transport. *Sci. Rep.* **9**, 1–9 (2019).
- 351 16. Thamaga, K. H. & Dube, T. Remote sensing of invasive water hyacinth (*Eichhornia crassipes*):
352 A review on applications and challenges. *Remote Sensing Applications: Society and*
353 *Environment* vol. 10 36–46 (2018).
- 354 17. CABI. *Eichhornia crassipes* (water hyacinth). In: *Invasive Species Compendium*. Wallingford,
355 UK: CAB International. (2020).
- 356 18. IUCN. Water Hyacinth , an Invasive Plant in the Lake Tanganyika Basin. (2017).
- 357 19. EDDMapS. Early Detection & Distribution Mapping System. *The University of Georgia - Center*
358 *for Invasive Species and Ecosystem Health* <http://www.eddmaps.org/> (2020).
- 359 20. Sharma, A., Aggarwal, N. K., Saini, A. & Yadav, A. Beyond biocontrol: Water hyacinth-
360 Opportunities and challenges. *J. Environ. Sci. Technol.* **9**, 26–48 (2016).
- 361 21. Ongore, C. O., Aura, C. M., Ogari, Z., Njiru, J. M. & Nyamweya, C. S. Spatial-temporal
362 dynamics of water hyacinth, *Eichhornia crassipes* (Mart.) and other macrophytes and their
363 impact on fisheries in Lake Victoria, Kenya. *J. Great Lakes Res.* **44**, 1273–1280 (2018).
- 364 22. Dogliotti, A. I., Gossn, J. I., Vanhellefont, Q. & Ruddick, K. G. Detecting and Quantifying a
365 Massive Invasion of Floating Aquatic Plants in the R í o de la Plata Turbid Waters Using High
366 Spatial Resolution Ocean Color Imagery. *Remote Sens.* (2018) doi:10.3390/rs10071140.
- 367 23. Lebreton, L. C. M. *et al.* River plastic emissions to the world's oceans. *Nat. Commun.* **8**, 1–10
368 (2017).
- 369 24. Nguyen, T. T. N. *et al.* Nutrient budgets in the Saigon–Dongnai River basin: Past to future
370 inputs from the developing Ho Chi Minh megacity (Vietnam). *River Res. Appl.* **36**, 974–990
371 (2020).
- 372 25. van Emmerik, T. *et al.* A Methodology to Characterize Riverine Macroplastic Emission Into the
373 Ocean. *Front. Mar. Sci.* **5**, 372 (2018).
- 374 26. van Emmerik, T. *et al.* Manila River Mouths Act as Temporary Sinks for Macroplastic Pollution.
375 *Front. Mar. Sci.* **7**, 545812 (2020).
- 376 27. Geraeds, M., van Emmerik, T., de Vries, R. & bin Ab Razak, M. S. Riverine plastic litter
377 monitoring using Unmanned Aerial Vehicles (UAVs). *Remote Sens.* **11**, 6–8 (2019).
- 378 28. González-Fernández, D. & Hanke, G. Toward a harmonized approach for monitoring of riverine
379 floating macro litter inputs to the marine environment. *Front. Mar. Sci.* **4**, (2017).

- 380 29. Dutta, A. & Zisserman, A. *The VIA Annotation Software for Images, Audio and Video*.
381 <http://www.robots.ox.ac.uk/> (2019).
- 382 30. Lahens, L. *et al.* Macroplastic and microplastic contamination assessment of a tropical river
383 (Saigon River, Vietnam) transversed by a developing megacity. *Environ. Pollut.* **236**, 661–671
384 (2018).
- 385 31. Biermann, L., Clewley, D., Martinez-Vicente, V. & Topouzelis, K. Finding Plastic Patches in
386 Coastal Waters using Optical Satellite Data. *Sci. Rep.* **10**, (2020).
- 387 32. Martin, C., Almahasheer, H. & Duarte, C. M. Mangrove forests as traps for marine litter.
388 *Environ. Pollut.* **247**, 499–508 (2019).
- 389 33. Liro, M., van Emmerik, T., Wyzga, B., Liro, J. & Mikuś, P. Macroplastic storage and
390 remobilization in rivers. *Water (Switzerland)* **12**, 22–29 (2020).

391

392

393

394

395

396

397

398

399

400

401

402

403

404

405

406

407

408

409 **Supporting Information to** “Plastic plants: Water hyacinths as driver of plastic transport in tropical
410 rivers”

411 **MANUSCRIPT TITLE:** Plastic plants: Water hyacinths as driver of plastic transport in tropical rivers

412 **AUTHORS:** Louise Schreyers^{1*}, Tim van Emmerik¹, Thanh Luan Nguyen², Evelien Castrop¹, Ngoc-Anh
413 Phung³, Thuy-Chung Kieu-Le^{3,4}, Emilie Strady⁵, Lauren Biermann⁶, Martine van der Ploeg¹

414 ¹Hydrology and Quantitative Water Management Group, Wageningen University, Wageningen, The
415 Netherlands

416 ²École Polytechnique de Montréal, Montréal, Canada

417 ³Ho Chi Minh City University of Technology (HCMUT), Ho Chi Minh City, Vietnam

418 ⁴Vietnam National University Ho Chi Minh City, Ho Chi Minh City, Vietnam

419 ⁵Aix-Marseille University, Mediterranean Institute of Oceanography (MIO), Marseille, Université de
420 Toulon, CNRS/IRD, France

421 ⁶Plymouth Marine Laboratory, Prospect Place, Plymouth, UK

422 *Corresponding author

423 **No of figures:** 2

424 **No of pages:** 4

425 **Text S1 Calculation and extrapolation of plastic flux based on visual counting**

426 Plastic fluxes were estimated as follow:

427
$$P_i = \frac{N_{h,i}}{t_{h,i}} + \frac{N_{f,i}}{t_{f,i}}$$

428 With total plastic flux P_i [items/min] for segment i , counted items inside the hyacinth $N_{h,i}$ during
429 observation time $t_{h,i}$ [min] for segment i , and counted free-floating items $N_{f,i}$ during observation time $t_{f,i}$
430 [min] or segment i .

431 The total plastic flux for the entire river width P_{tot} was estimated using

432
$$P_{tot} = \left(\sum_{i=1,2,3}^n \frac{P_i}{w_i} \right) \cdot W$$

433 With observation width of each segment w_i and total river width W .

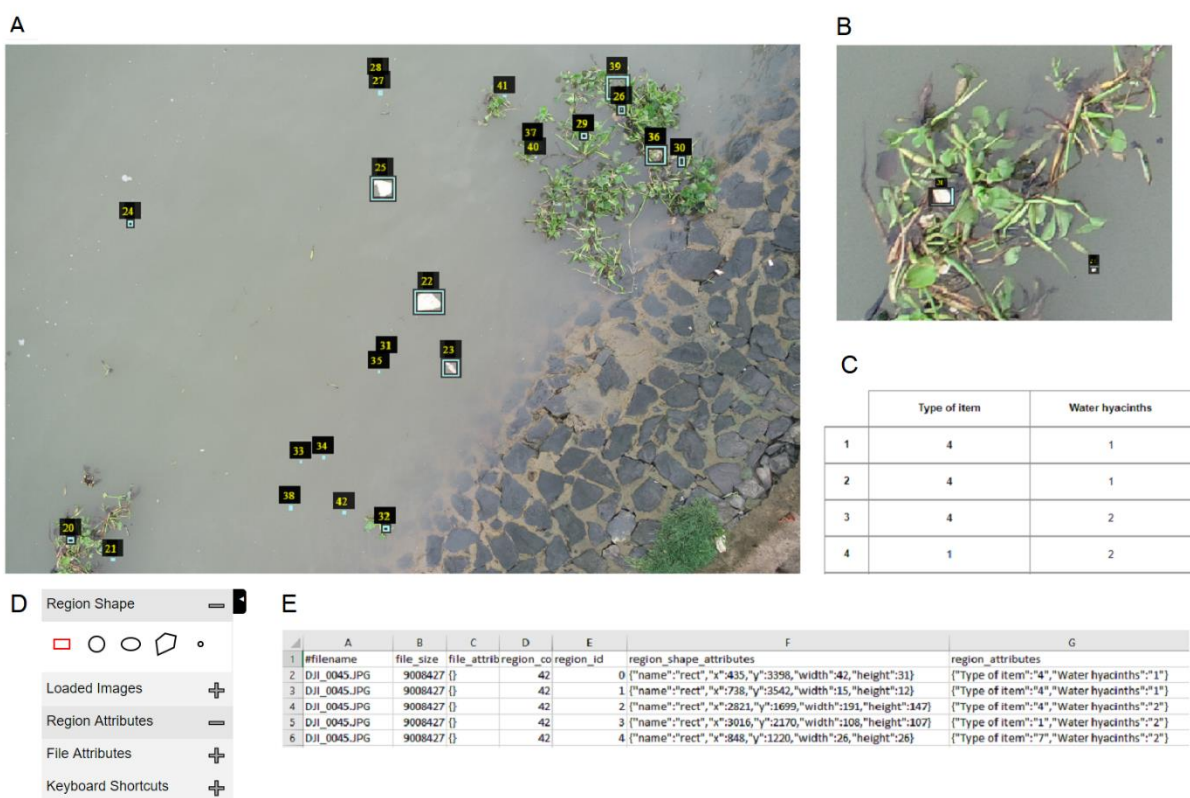
434 **Text S2 – Data acquisition of UAV images**

435 The DJI Phantom 4 Pro UAV has a FC6310 camera, equipped with a one-inch CMOS sensor with a
436 maximum resolution of 20 megapixels. This drone has a good camera resolution (5472 x 3648 pixels)
437 and two tracking system – GPS and GLONASS – for localization.

438 The flights were programmed using the DJI GS Pro App. We defined 22 waypoints every 15 m. Overall,
439 the flights covered the full width of the river. Precautions were taken to minimize blurry images: a ‘stop
440 and go’ mode was chosen, the camera shot interval was set at 2 seconds (the highest possible for the
441 Phantom 4 Pro) and the autofocus mode was disabled. The hovering time for each waypoint was set at

442 14 seconds, to stabilize the device before shooting several images. The images were captured at nadir,
 443 i.e. perpendicular ($90^\circ \pm 0.02^\circ$) to the direction of the flight, to facilitate surface calculations. The drone
 444 operated automatically, from take-off to landing. The memorization of the flight plans allowed several
 445 scans along the two river transects defined. Each flight lasted approximately ten minutes. The flights
 446 were carried out by qualified UAV pilots following Vietnamese aviation rules.

447 The aerial surveys were conducted at two altitudes. The scans along the river transects were scheduled
 448 at 5 m from the chart datum (derived from the lowest astronomical tide). A few images ($n = 11$) were
 449 captured at 15 m of altitude above the chart datum, usually in the middle section of the river. These
 450 images were retained for items count analysis and discarded for statistics on spatial distribution and
 451 temporal variability.

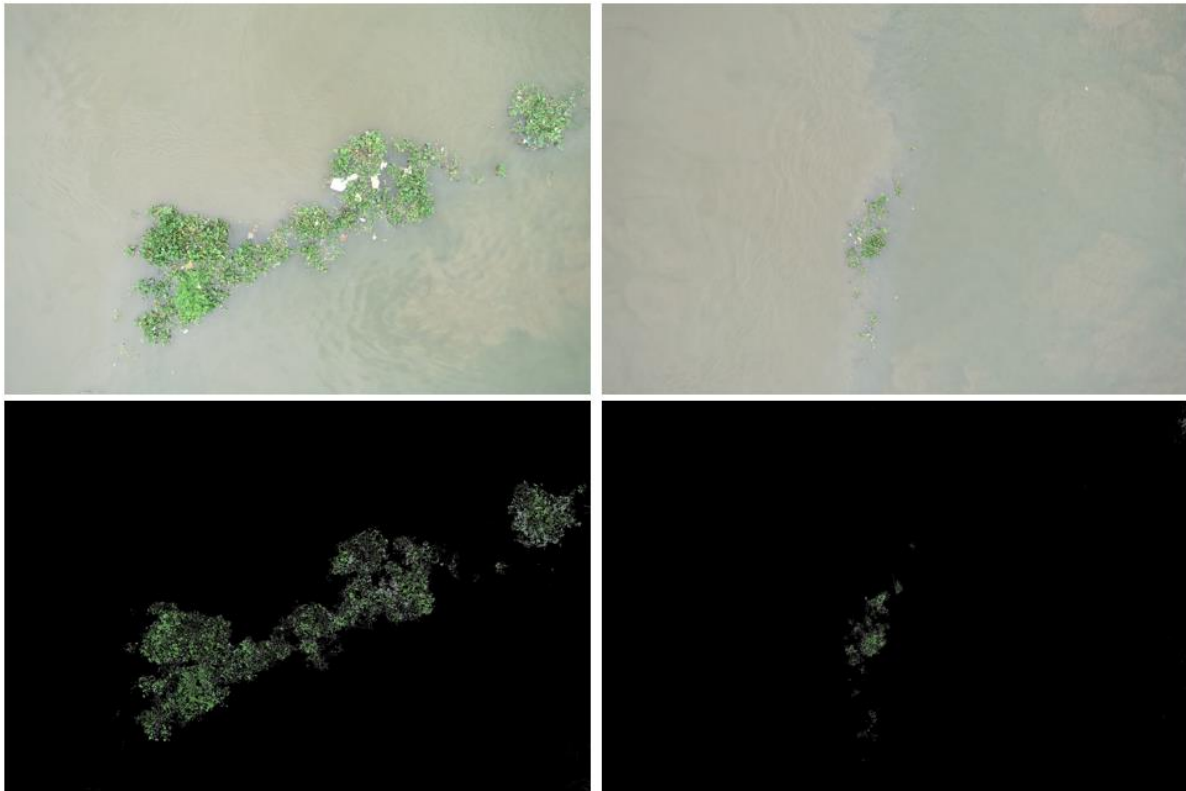


452
 453 **Figure S1.** VIA tool web-browser interface. The main view window (A) shows a photograph, taken close
 454 to the riverbank, with typical small patches of water hyacinths with a few items aggregated. The zoom-
 455 in function (B) enables closer inspection of the items and the drawing of rectangular bounding box. The
 456 region attribute panel (C) shows the main attributes filled in after the identification of an item. (D) shows
 457 the main functions available to the user. (E) is a sample .csv file with all the attributes per item annotated.

458 **Text S3 Color filtering and area estimates**

459 The Open CV library is used for computer vision and color filtering operations. The color segmentation
 460 functions enable to identify regions with a specific color, using the RGB channels of images. In this case,
 461 the upper and lower thresholds in the RGB color space were defined for masking the green areas
 462 corresponding to floating vegetation (fig. S2). Due to differences in the background reflectance,

463 luminosity, various shades of green of the vegetation, the thresholders values had to be adjusted per
464 image or group of images. This was done by trial and error tests.



465
466 **Figure S2.** Examples of images with visible large patches of water hyacinths (top) and color filtering
467 outputs for detecting floating hyacinth patches (bottom).

468 A total of 86 images were initially analyzed using color filtering, corresponding to the images with visible
469 floating vegetation. From this collection, images with very small organic debris components – such as a
470 floating branch or leaf - and those where the color segmentation did not perform well were discarded (n
471 = 11). These included aerial images showing large number of false positives detected in open water or
472 riverbanks. A final collection of 75 images were thus retained for color segmentation analysis.

473 Given the variations in the water level due to the tidal influence, the actual flying elevation from the drone
474 standpoint (at a time t) H_f was adjusted by correcting the flying elevation from chart datum as below:

475

$$H_f = H - H_s$$

476 Where H is the elevation from chart datum and H_s is the water height registered at a time t. The water
477 elevation was manually measured before the take-off of the drone and considered stable throughout the
478 whole flight duration (approximately 10 minutes).

479 Once the flying altitude was determined, the ground sampling distance (d_g) was calculated as follows:

480

$$d_g = \frac{S_w \times H_f \times 100}{F_r \times w_i}$$

481 Where S_w is the sensor width of the camera, H_f is the flight height in meters, F_r is the focal length of
482 the camera in millimeters and w_i is the image width in pixels. The d_g was determined for each drone
483 scan and for the set of images taken at a higher elevation. For the whole image collection, an average
484 d_g of 0.175 cm/pixel was found.

485